J Solid State Eletrochem (2004) 8: 352–359
DOI 10.1007/s10008-003-0470-0

ORIGINAL PAPER

Kazimierz Darowicki · Juliusz Orlikowski
Anna Arutunow

Dynamic electrochemical impedance spectroscopy measurements of passive layer cracking under static tensile stresses

Received: 15 June 2003 / Accepted: 22 October 2003 / Published online: 14 January 2004

Abstract Electrochemical impedance spectroscopy allows the examination of corrosion susceptibility and resistance for different construction materials, in particular the determination of the properties of their passive films. This technique makes possible the analysis of electrochemical processes in time domain, including rapid phenomena such as changes in the properties of passive films, but it has never been used for passive layer cracking examination. In many cases, fracture of the passive film under tensile stresses leads to stress corrosion cracking. Therefore, investigations of passive layer cracking on austenitic stainless steels under tensile stresses facilitate the understanding of the mechanism of stress corrosion cracking in these common engineering materials. The effect of static tensile stresses on the passive film cracking behaviour of type 304L stainless steel immersed in 0.5 M NaCl solution at room temperature has been investigated. This paper presents the impedance spectra obtained for 304L stainless steel samples at different potential values.

Keywords Austenitic stainless steels · Dynamic electrochemical impedance spectroscopy · Passive layer cracking · Stress corrosion cracking · Tensile stresses

Introduction

Classical stress corrosion cracking (SCC) investigations comprise of electrochemical and mechanical measurements and metallographic examinations. Electrochemical measurements are used to estimate the SCC risk but are also helpful in acceleration of that process [1]. The problem is that such investigations do not give information about the dynamics of the initiation and propagation of the crack path. Potentiostatic measurements are the easiest way and the dynamics of the current changes reflects the SCC process. The use of the potentiodynamic technique developed knowledge of the SCC mechanism [2, 3, 4]. Thanks to these kinds of measurements, it is possible to allocate values of the characteristic potentials for SCC. However, at present, the electrochemical techniques do not make possible the exact estimation of SCC in the time domain. This is the reason why the analysis of the SCC mechanism is usually obtained by means of microscopic analysis [5, 6]. The great evolution of mathematical analysing techniques enabled a breakthrough in electrochemical measurements [7]. The use of joint time–frequency analysis facilitated examination of impedance measurements in the time domain, but it was never used for SCC research.

Classical impedance measurements [8, 9] are carried out using a sinusoidal voltage perturbation signal with a deterministic frequency. After measuring the real and imaginary parts of the impedance for frequency ω_i, the frequency is changed to the value ω_{i+1} and the impedance measurement is repeated. One obtains a sequence of conjugated impedance values determined for the assumed frequencies. This method is named "frequency by frequency".

If the electrode process does not depend on time and if the surface area is constant, the averaged value of the admittance/impedance is equal to its instantaneous value. The situation is more complicated if the investigated process is carried out under non-stationary conditions. In this case, the stability condition is not fulfilled and the classical "frequency by frequency" impedance measurement gives inadequate results. Inadequate impedance results are also obtained for the system in which the surface area changes with time.

Contribution to the 3rd Baltic Conference on Electrochemistry, Gdansk-Sobieszewo, Poland, 23–26 April 2003

Dedicated to the memory of Harry B. Mark, Jr. (28 February 1934–3 March 2003)

K. Darowicki (✉) · J. Orlikowski · A. Arutunow
Department of Anticorrosion Technology,
Gdansk University of Technology,
Narutowicza 11/12 Str.,
80-952 Gdansk, Poland
E-mail: zak@chem.pg.gda.pl

Recently, Darowicki and co-workers [10, 11, 12] elaborated a new dynamic impedance technique. This technique gives the possibility of determinating the instantaneous impedance characteristics of the passive layer cracking process. Rupture of the passive layer is considered as one of the most common initiation stages of SCC [13]. Electrochemical parameters obtained from impedance spectra can provide new information about changes in the properties of the passive layers in such dynamic conditions.

The aim of this paper is to demonstrate that the new Dynamic Electrochemical Impedance Spectroscopy (DEIS) can be used in passive layer cracking research. In many cases, fracture of the passive film under tensile stresses leads to stress corrosion cracking.

Experimental

The examined samples were made of 304L stainless steel in the form of bars. The composition of 304L stainless steel is given in Table 1. The samples were mounted in a measurement cell and then in a static tensile testing machine. The applied static tensile stresses were equal to 380 MPa. The middle part of the investigated samples had been narrowed and that was the working specimen. Characteristic dimensions of a specimen and the measurement cell are presented in Fig. 1. The narrowed part of the samples was exposed to an electrolytic environment. The geometric area of the working electrode was equal to 3.1415 mm^2. The rest of the specimen was isolated from the environment. A silver/silver chloride electrode was used as the reference electrode and the auxiliary electrode was made of platinum net. The electrolyte environment used in the investigations was 0.5 M NaCl solution. The time of the impedance measurements was correlated with the static tensile process.

The measurements were performed by means of the DEIS technique, in which the perturbation is a multi-sine signal. This method is general and allows the analysis of impedance spectra in a joint time–frequency domain. The perturbation and response signals are registered continuously during the measurement. Although the measurement methodology is not new, the analysing procedure differs from fast Fourier transformation. The analysing window function is employed to cut a fragment out of the recorded register. In the next step this segment is subjected to the regular Fourier transformation and an instantaneous spectrum is determined. The spectrum is averaged over the time range equal to the length of the analysing window. By moving the window and repeating the analysing procedure over the entire register, we receive a set of instantaneous impedance spectra reflecting the dynamics of the examined process. Accordingly, a complete characteristic of the system's impedance over time can be accessed.

The range of analysed frequencies has to reflect the dynamics of the electrochemical process under investigation. Generally, faster electrochemical process requires higher frequencies to be applied. So the lowest frequency must be limited, owing to substantial system dynamics. Its value has to be higher that the rate of the investigated system changes. The higher frequency value is defined by the technical analysing ability (the size of the obtained data register), the computing power of the equipment and the sampling frequency.

Table 1 Normalized chemical composition of AISI 304L (average values)

C	Mn	Si	P	S	Cr	Ni	Fe
≤ 0.03%	≤ 2.0%	≤ 1.0%	≤ 0.04%	≤ 0.03%	17–19%	9–11%	Balance

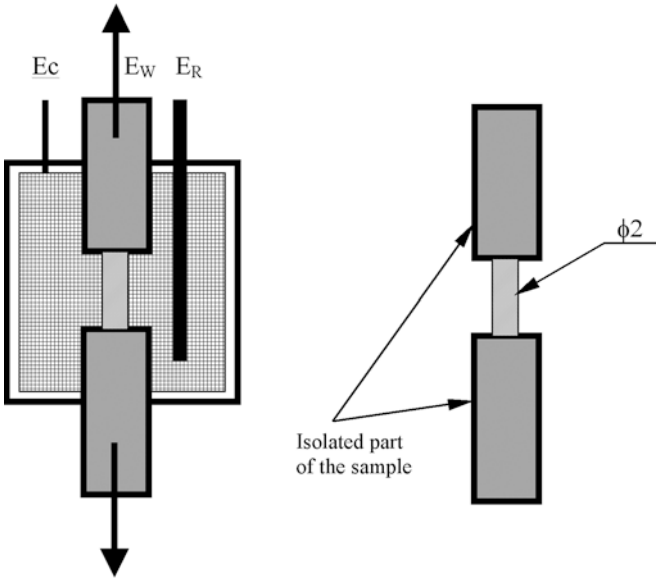

Fig. 1 Measurement cell and characteristic dimensions of the examined samples

The measurement set-up consisted of an ELPAN EP20A potentiostat and a National Instruments AT-MIO-16E-1 card generating the perturbation signal. The amplitudes of all elementary sinusoidal signals were equal to $u_0 = 8$ mV. Two National Instruments PCI-6052E cards driven by one signal registered the voltage perturbation and current response signals. The sampling frequency of 12,288 Hz resulted from the card settings at our disposal. DEIS measurements were conducted in the frequency range of 2640 to 3 Hz for different potential values of $E = -0.300$, -0.200, -0.150 and 0.000 V. The time resolution was equal to 0.98 s.

Results and discussion

Figure 2 illustrates the exemplary stress–elongation dependence for the examined 304L stainless steel obtained during the slow strain tests. This diagram is presented in order to note that the applied static load exceeds the yield strength for this steel. The tensile strength takes an average value in the range 500–600 MPa.

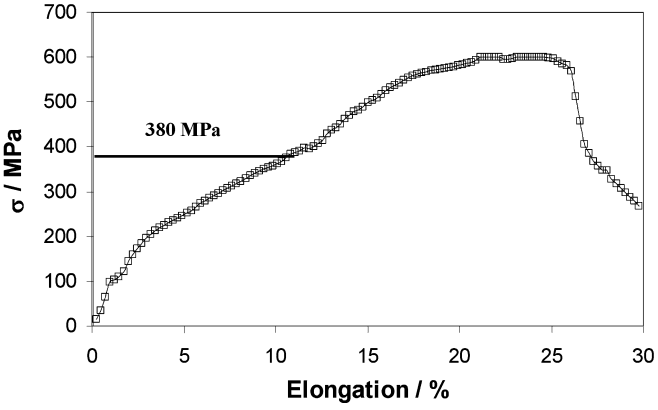

Fig. 2 Stress as a function of elongation for 304L stainless steel

Impedance spectra received from the measurements as a function of time are shown in Fig. 3. It should be noted that these spectra were registered for the applied frequency range, but they show the instantaneous changes in the passive layer and not the exact time of the passive layer cracking. Emphasis was put on obtaining a better frequency resolution than a time one in order to detect more detailed dynamic changes in the passive layer during the experiment.

Each diagram in Fig. 3 presents spectra recorded for different potential values. It can be clearly noticed that when the potential increases in the anodic direction, the moment of the passive layer cracking can be seen more distinctly. In Fig. 3a ($E_{COR} = -0.300$ V) we cannot observe any changes in the impedance spectra because the passive layer did not break during the measurement.

Such changes are more noticeable in Fig. 3b for the potential value $E = -0.200$ V. The spectra in Fig. 3c and Fig. 3d are distinguished from the previous ones. For the potential $E = -0.150$ V the repassivation phenomenon can be observed after cracking of the passive layer. In Fig. 3d the spectra in the first region refer to the stable passive state and have diffusion character (straight lines), whilst the others reflect the active state of investigated stainless steel (semicircles), that is, after passive layer cracking. No repassivation was detected in that case. Thus, it can be observed that moment of the passive layer cracking was detected.

In order to provide a detailed description of the investigated process, impedance spectra have been illustrated in Fig. 4 as Bode plots for the potential value of 0.000 V.

Elementary analysis of the impedance spectra proved that in the investigated potential range the process run can be described by the equivalent circuit presented in Fig. 5a. Owing to limited range of applied measurement frequencies, the electrolyte resistance R_8 could not be assessed precisely. As a result, the determination of the C'_2 and C'_7 values was not possible. Consequently, the initial equivalent circuit had to be simplified to the form illustrated in Fig. 5b. Nevertheless, such an equivalent circuit demonstrated very good correlation with the experimental impedance spectra over the whole potential range. Experimental impedance spectra were correlated with this circuit based on the method proposed by Boukamp [14].

In accordance with this equivalent circuit (Fig. 5b), the passive layer comprises of an internal sublayer adhering to the metal base and an outer sublayer remaining in contact with the electrolyte solution. It was not possible to estimate the electrolyte resistance values precisely because of the limited range of the frequencies employed. The capacitance of the internal part of the passive layer is described by C_2, which is the combined capacitance of the internal part of the passive layer and the electric double layer at the uncovered metal surface. Parameter C_4 refers to the capacitance of the outer part

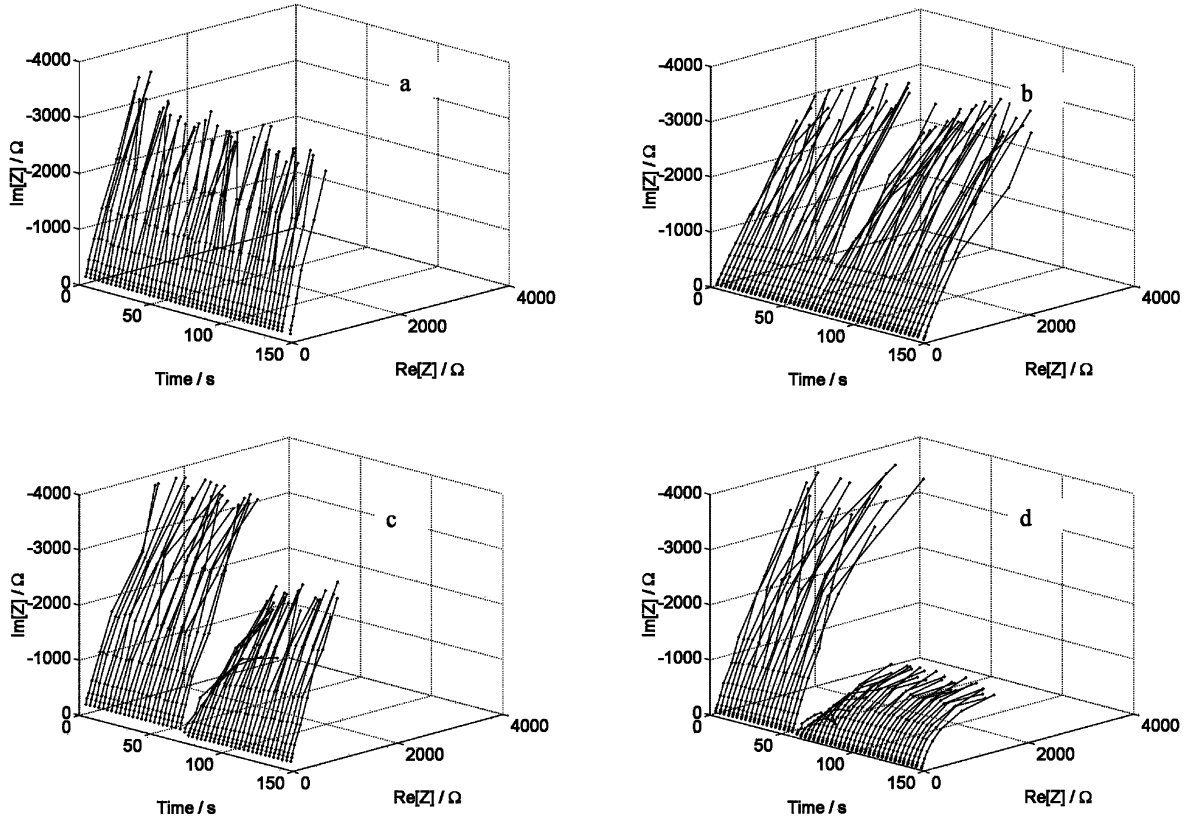

Fig. 3 Diagram of the impedance spectra of SCC versus time: (**a**) $E = -0.300$ V, (**b**) $E = -0.200$ V, (**c**) $E = -0.150$ V, (**d**) $E = 0.000$ V

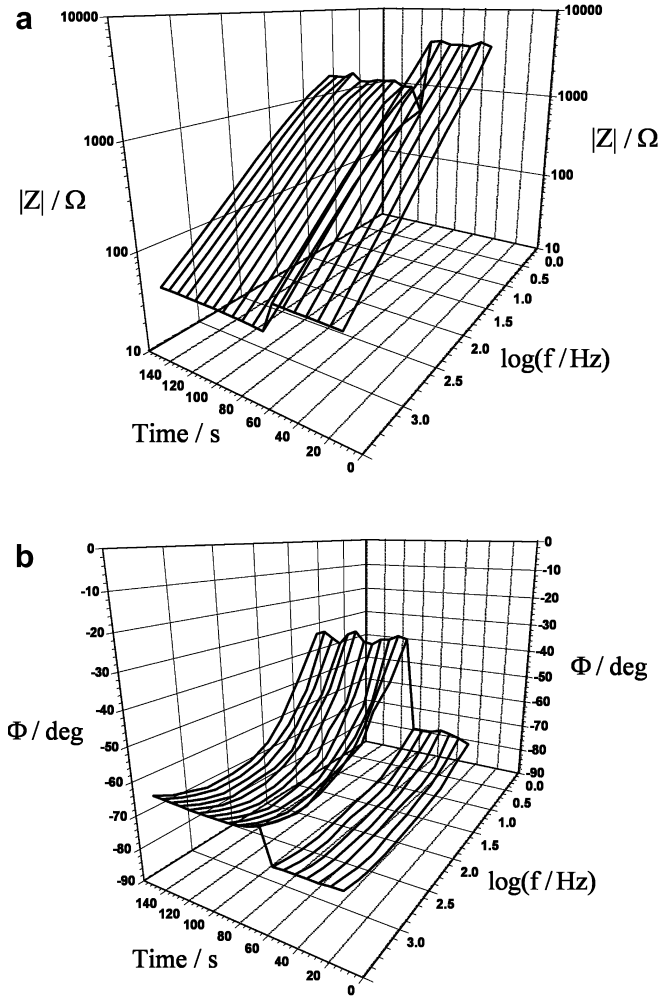

Fig. 4 Diagram of Bode plots as a function of time for a potential of 0 V

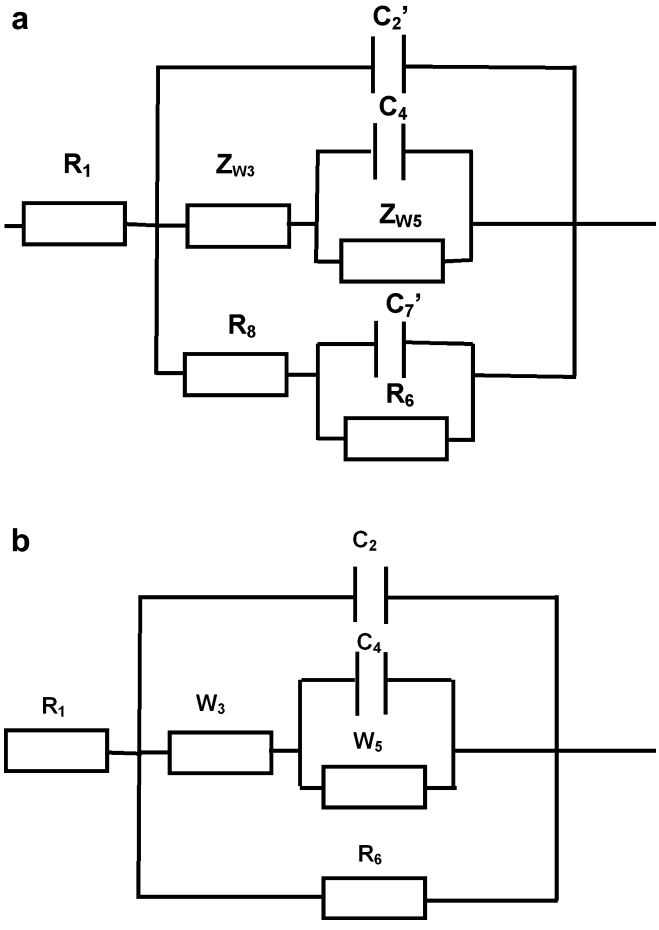

Fig. 5a, b Equivalent circuits. (**a**) Initial version: R_1 = electrolyte resistance; W_3 = Warburg coefficient of the internal part of the passive layer; C_2' = capacitance of the internal part of the passive layer; C_4 = capacitance of the outer part of the passive layer; W_5 = Warburg coefficient of the outer part of the passive layer; R_8 = electrolyte resistance occurring in the cracks of the passive layer; C_7' = capacitance of the electric double layer at the uncovered metal surface; R_6 = charge transfer resistance. (**b**) Simplified version: R_1 = electrolyte resistance; C_2 = capacitance of the internal (crystalline) part of the passive layer; W_3 = Warburg coefficient of the internal (crystalline) part of the passive layer; C_4 = capacitance of the outer (amorphous) part of the passive layer; W_5 = Warburg coefficient of the outer (amorphous) part of the passive layer; R_6 = charge transfer resistance

of the passive layer. Ions and defects transport through the internal sublayer via diffusion and are described by the Warburg coefficient W_3. Ions and defects transport through the outer sublayer via diffusion also and this is described by the Warburg coefficient W_5. In the investigated potential range, a new branch arises in the equivalent circuit, which reflects the electron charge transfer. The charge transfer resistance R_6 is a measure of the resistance of the transfer electrons caused by electrode reactions, which occur inside the crack on the bare active metal surface. Owing to the limited frequency range, the capacitance of the electric double layer inside the crack, which should be connected in parallel with R_6, could not be calculated directly and C_2 was measured instead.

Part of the equivalent circuit that contains C_2, W_3, C_4 and W_5 refers to the stable passive state and can be confirmed by the theoretical expectations of Macdonald [9], Jüttner et al. [15] and MacDoughall and Graham [16].

From each impedance spectrum the DC current component was filtered. As a result, the dependence between current and time was obtained and is illustrated in Fig. 6. In this diagram the straight line indicates the time (after about 47 s) for which the investigated system started working under a static load equal to 380 MPa. For such a time, any current changes cannot be seen. An increase in current values can be observed just after about 65 s for all examined potential values except the corrosion potential. The same time of 18 s after the stress imposition for the crack formation, independent of the potential, means a purely mechanical origin of the crack, rather than an electrochemical one. A distinct current increase was found only for the potentials $E = 0.000$ V and $E = -0.150$ V, and for the potential $E = -0.200$ V such an increase was slight. The increase in current values is considerable when the potential rises in

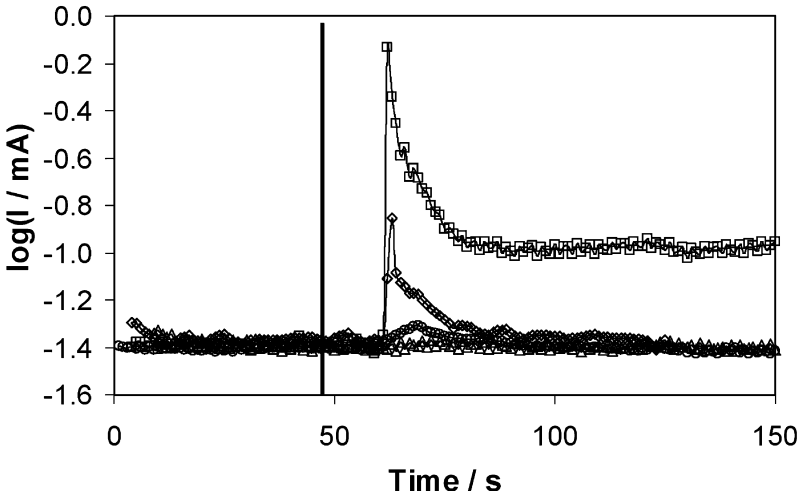

Fig. 6 Diagram of current changes as a function of time for 304L stainless steel: $E = -0.300$ V (*triangles*), $E = -0.200$ V (*circles*), $E = -0.150$ V (*diamonds*), $E = 0.000$V (*squares*)

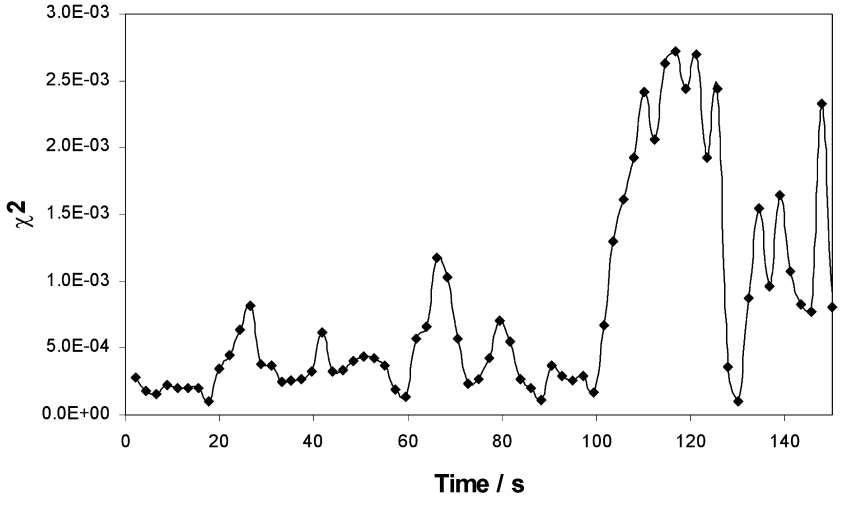

Fig. 7 Diagram of impedance results fitting accuracy using the NLLS-fit procedure for a potential of 0 V

the anodic direction. Passive layer cracking can explain the increase in the current values. In the case of $E = 0.000$ V, the current value maintains at the high level after the crack of the passive layer, which cannot be seen for the other potentials. It can be accounted for by the fact that the repassivation phenomenon does not occur after the crack of the passive layer for the lower level of the potential. This can be confirmed by the spectra presented in Fig. 3d. On the basis of the received data, it can be concluded that the passive layer cracking does not appear directly after the applied static load but after about 18 s from that moment.

On the basis of the presented equivalent circuit, the analysis of the impedance spectra was performed. Figure 7 illustrates the fitting accuracy of the impedance dependence using the employed equivalent circuit for $E = 0.000$ V.

In Fig. 8 the dependence between the charge transfer resistance (R_6) and the time for the potentials $E = -0.200$, -0.150 and 0.000 V is presented. In the case of the corrosion potential, the charge transfer resistance values could not be allocated.

For the potential $E = 0.000$ V the R_6 values were allocated and achieved a constant level after some time, which means that the repassivation process did not appear and the samples were in the active state until the end of the experiment. For the potentials $E = -0.200$ V and $E = -0.150$ V the R_6 values were allocated for the period of time just after the crack of the passive layer. Moreover, in these cases the repassivation process appeared and in the end the steel was in the passive state. The values of the charge transfer resistance are well

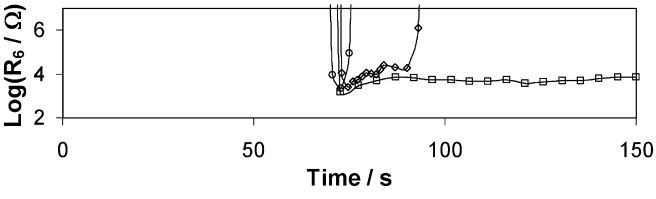

Fig. 8 Time dependence of the charge transfer resistance (R_6) for 304L stainless steel: $E = -0.200$ V (*circles*), $E = -0.150$ V (*diamonds*), $E = 0.000$ V (*squares*)

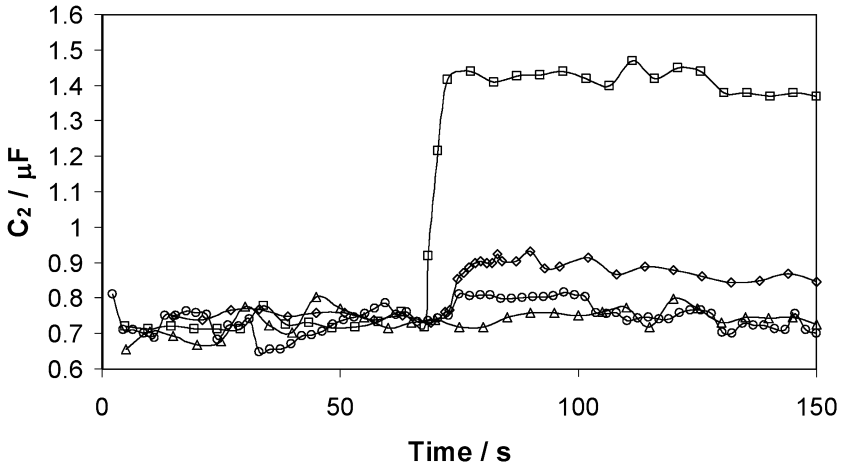

Fig. 9 Time dependence of the C_2 parameter for 304L stainless steel: $E=-0.300$ V (*triangles*), $E=-0.200$ V (*circles*), $E=-0.150$ V (*diamonds*), $E=0.000$ V (*squares*)

correlated with the current values and impedance spectra (see Fig. 3 and Fig. 6).

Figure 9 presents the dependence between the capacitance of the internal part of the passive layer (C_2) as a function of the measurement time for particular potential values. For the potentials $E=0.000$ V and $E=-0.150$ V, a distinct increase in C_2 values can be noticed for the time at about 65 s; for the corrosion potential, no changes in this parameter were observed during the measurement time. On that basis it can be said that the change of the C_2 values strongly depends on the potential. According to the proposed equivalent circuit (see Fig. 5), parameter C_2 represents the capacitance of the internal (compact) crystalline part of the passive layer. This capacitance is connected with the dielectric coefficient of the oxides. As a result of static tensile stresses and aggressive electrochemical conditions, the process of passive layer cracking can proceed. The water content in the oxide structure can increase in such conditions. This can contribute to the increase in C_2 values due to different dielectric coefficients for water and oxide. On such a basis it can be concluded that the increase in C_2 values can be explained by the crack of the compact part of the passive layer. Furthermore, the C_2 parameter is strongly connected with the thickness of the passive layer. Accordingly, the increase in C_2 values is due to the decrease in its thickness. As in Fig. 6, the process of passive layer cracking did not occur at the moment of static load (about 47 s) but just after a couple of seconds from that moment. The data illustrated in Fig. 9 indicate that this process is very rapid so it cannot be measured by means of the classical impedance technique "frequency by frequency". Furthermore, analysis of the changes in the capacitance of the internal part of the passive layer makes it possible to monitor the passive layer cracking process during the initiation stage of the stress corrosion cracking.

In Fig. 10 the time dependence of the Warburg coefficient (W_3) of the compact crystalline part of the passive layer is presented for particular potentials. On the basis of this diagram it can be corroborated that for the potentials $E=0.000$ V and $E=-0.150$ V the W_3 values decrease for the time $t=65$ s. In accordance with earlier information for the time $t=65$ s, the process of passive layer cracking for the potentials $E=0.000$ V and $E=-0.150$ V was observed. This can be confirmed by the dependences shown in Fig. 6 and Fig. 9. The W_3 parameter is strongly connected with the diffusion

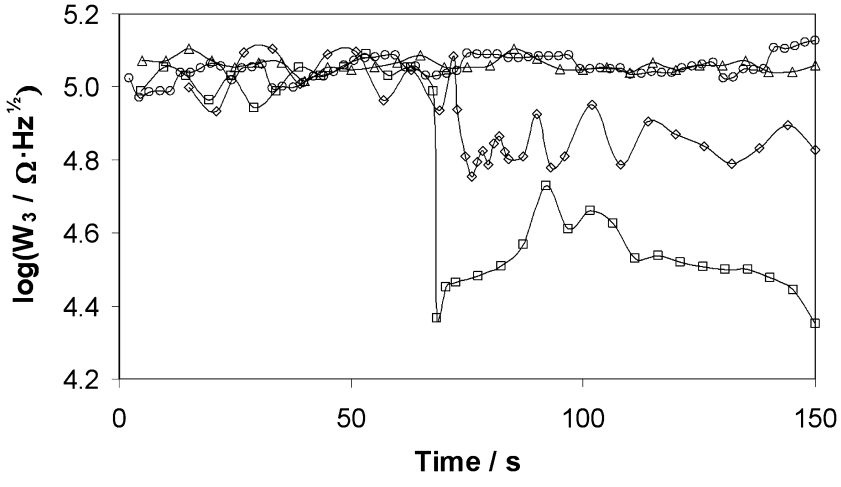

Fig. 10 Dependence between W_3 and time for 304L stainless steel: $E=-0.300$ V (*triangles*), $E=-0.200$ V (*circles*), $E=-0.150$ V (*diamonds*), $E=0.000$ V (*squares*)

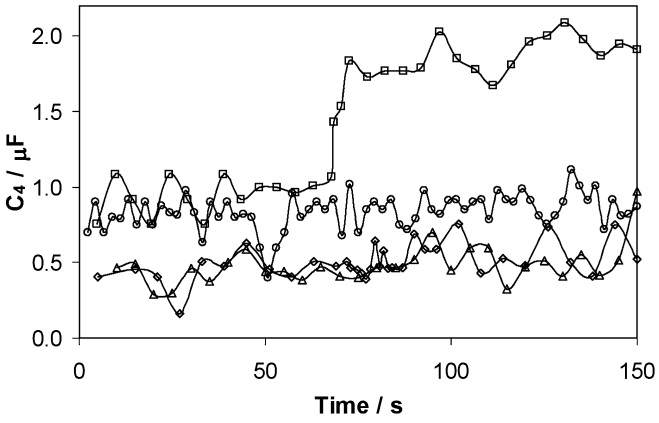

Fig. 11 The curve of C_4 changes with time for 304L stainless steel: $E=-0.300$ V (*triangles*), $E=-0.200$ V (*circles*), $E=-0.150$ V (*diamonds*), $E=0.000$ V (*squares*)

resistance through the compact part of the passive layer. Moreover, with an decrease in W_3 values the diffusion resistance decreases as well, because of less thinning of the passive layer. Therefore, the decrease in W_3 values for the potentials $E=0.000$ V and $E=-0.150$ V characterizes the process of passive layer cracking. This is well correlated with the C_2 values (see Fig. 9), which increase as a function of the measurement time; at the same time the thickness of the passive layer decreases. On the other hand, for the potentials $E=-0.200$ V and $E=-0.300$ V, no changes in the W_3 parameter values were observed.

Figure 11 presents the capacitance of the outer (amorphous) part of the passive layer (C_4) as a function of the measurement time for the examined potential values. In agreement with the physical sense of the accepted equivalent circuit (see Fig. 5), the C_4 parameter characterizes the outer (hydrated) part of the passive layer. Data presented in Fig. 11 indicate that only for the potential $E=0.000$ V does the increase in C_4 values occur as a function of the measurement time. For other potentials, any changes in the C_4 values as a function of measurement time were not corroborated. An increase in C_4 values can be accounted for an increase in the water content in the passive layer structure but also for the fact that the barrier properties become worse. The hydrated part of the passive layer is not located in the direct vicinity of the steel surface, so its changes with the electrochemical conditions will not be as direct as in the case of the compact part of the passive layer. As a result, the C_4 parameter is not good enough for passive layer estimation. The increase in C_4 values only for the potential $E=0.000$ V can be explained by the limited dependence of this parameter on the electrochemical conditions.

In Fig. 12 the time dependence of the Warburg coefficient of the outer part of the passive layer (W_5) for the examined potentials is illustrated. The data indicate that there is no correlation between W_5 values and measurement time and the potential level. Therefore this parameter cannot be used for passive layer assessment under static tensile stresses.

Conclusions

The phenomenon of passive layer cracking is very rapid and application of the classical impedance technique (''frequency by frequency'') does not give precise results. The use of DEIS makes possible the DC detection which is passing through the sample under examination. In the case of classical impedance measurements, it is necessary to carry out additional DC measurements.

On the basis of the impedance measurements, it can be stated that the applied DEIS enables the assessment of the passive layer under static tensile stresses. Investigations show that static tensile stresses, an aggressive electrolyte environment and anodic polarization have a strong influence on the passive layers of the examined stainless steel. The process of passive layer cracking occurred for the potentials $E=-0.150$ V and $E=0.000$ V, whereas for $E=-0.200$ V and $E=-0.300$ V the cracking of the passive layer was not observed.

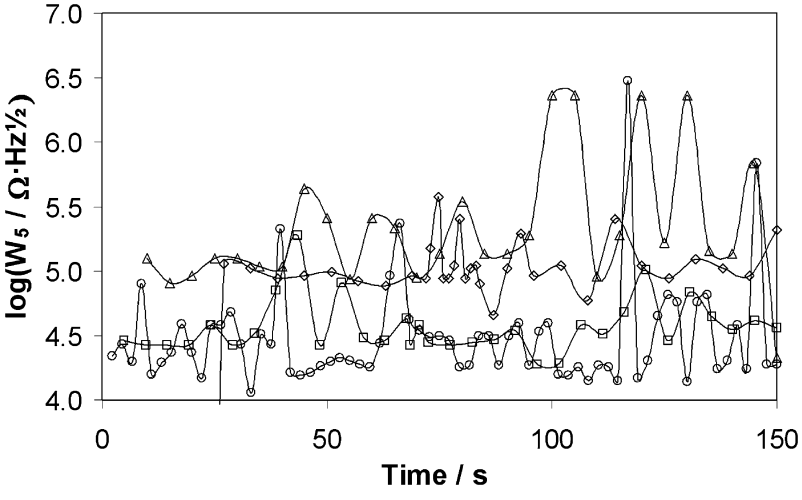

Fig. 12 The curve of W_5 changes with time for 304L stainless steel: $E=-0.300$ V (*triangles*), $E=-0.200$ V (*circles*), $E=-0.150$ V (*diamonds*), $E=0.000$ V (*squares*)

The analysis of the processes occurring inside the passive layer is possible in the time domain. It was recognized that the parameters of the equivalent circuit [the charge transfer resistance (R_6) and the capacitance of the internal part of the passive layer (C_2)] are the best reflections of the dynamics of the passive layer cracking. All the parameters of the equivalent circuit indicate there is a significant difference between the physical and electrochemical phenomena taking place within the outer and internal parts of the passive layer. It is also clear that cracking of the passive layer appeared after a certain period of time (about 18 s), not immediately after the application of the static tensile stresses. All the above suggest that passive layer cracking investigated by means of DEIS requires detailed research, taking into account all mechanical and electrochemical factors. Further results will be published on this subject in the following paper.

References

1. Haruna T, Toyota R (1997) Corros Sci 39:1873
2. Haruna T, Shibata T, Toyota R (1997) Corros Sci 39:1935
3. Kolamn D, Ford D, Butt D, Nelson T (1997) Corros Sci 39:2067
4. Cihal V, Stefec R (2001) Electrochim Acta 46:3867
5. Garcia C, Martin F, De Riedra P, Heredero J, Aparicio M (2001) Corros Sci 43:1519
6. Loria A (1982) J Met 34:16
7. Darowicki K (2000) J Electroanal Chem 486:101
8. Gabrielli C (1995) Identification of electrochemical processes by frequency response analysis. In: Technical report number 004/83. Farnborough, UK
9. Macdonald DD (1991) Application of electrochemical impedance spectroscopy in electrochemistry and corrosion science: In: Varma R, Selman JR (eds) Techniques for characterization of electrodes and electrochemical processes. Wiley, New York, pp 515–647
10. Darowicki K, Lentka G, Orlikowski J (2000) J Electroanal Chem 486:10
11. Darowicki K, Slepski P (2003) J Electroanal Chem 547:1
12. Darowicki K, Slepski P (2002) J Electroanal Chem 533:25
13. Newman RC (1995) Stress-corrosion cracking mechanisms. In: Marcus P, Oudar J (eds) Corrosion mechanisms in theory and practice. Dekker, New York, pp 311–372
14. Boukamp BA (1986) Solid State Ionics 20:31
15. Jüttner K, Lorenz WJ, Paatsch W (1989) Corros Sci 29:279
16. MacDoughall B, Graham MJ (1995) Growth and stability of passive films. In: Marcus P, Oudar J (eds) Corrosion mechanisms in theory and practice. Dekker, New York, pp 143–173